A ONE-DIMENSIONAL SIMULATION OF THE INTERACTION BETWEEN LAND SURFACE PROCESSES AND THE ATMOSPHERE

J. SIEBERT*, U. SIEVERS** and W. ZDUNKOWSKI
Institute for Atmospheric Physics, Johannes Gutenberg-University, Mainz, Germany

(Received in final form 1 August, 1991)

Abstract. A one-dimensional soil-vegetation model is developed for future incorporation into a mesoscale model. The interaction of land surface processes with the overlying atmosphere is treated in terms of three coupled balance equations describing the energy and moisture transfer at the ground and the energy state of the vegetation layer. For a complete description of the interaction, the coupled processes of heat and moisture transport within the soil are included as a multilayer soil model. As model verification, successful reproductions of the observed energy fluxes over vegetated surfaces from the HAPEX-MOBILHY experiment in southwestern France and from the LOTREX-10E/HIBE88 field experiment in Germany are presented. Finally, some sensitivity studies are performed and discussed in order to investigate the influence of different soil and vegetation types on the energy state of the atmosphere.

1. Introduction

Mesoscale and global climate models require an accurate description of the lower boundary conditions for the atmospheric equations. Various comprehensive investigations of the atmospheric boundary layer have shown that the redistribution of the incoming solar energy is strongly influenced by physical processes at the earth's surface. Therefore, it has become mandatory to incorporate the physical effects of the vegetation-soil system on the overlying atmosphere into climate models.

In the past few years, several authors have contributed to the important topic of parameterization of heat, mass and momentum exchange between a vegetation canopy and the overlying atmosphere, see, e.g., Crowan (1968), Thom (1972). This includes the evapotranspiration by leaves (e.g., Monteith, 1975) as well as the processes of heat and moisture transport within the soil (e.g., Philips (1957), Zdunkowski *et al.* (1975b), McCumber and Pielke (1981)). Coupled vegetation-soil models were developed by Deardorff (1978) with some important modifications-by Dickinson (1984). In a recent paper, Sellers *et al.* (1986) propose a comprehensive canopy model which calculates the physical properties of vegetation and their influence on the atmosphere. The complexity of the model requires a large number of empirical parameters and a high level of computational effort.

In this paper, a soil-canopy model is developed based on the work of Deardorff

* Sections of the present paper are part of a dissertation.
** Deutscher Wetterdienst, Zentralamt, 6050 Offenbach, Germany.

Boundary-Layer Meteorology **59**: 1–34, 1992.
© 1992 *Kluwer Academic Publishers. Printed in the Netherlands.*

and Dickinson. Their models, already including the essential physical effects of vegetation on the atmosphere, can be handled numerically in a very efficient way. While these authors applied the so-called force-restore method to approximate surface temperature and soil moisture, the present work introduces a fairly complete multilayer soil model which evolved from an earlier investigation by two of these authors (Sievers *et al.*, 1983). Unlike the soil model of McCumber and Pielke, the interaction of heat and moisture transport within the soil is explicitly considered by solving a system of two coupled differential equations for soil temperature and moisture content. Moreover, the water uptake by the root system is included.

The vegetation model uses the parameterization scheme suggested by Deardorff. Nevertheless, the determination of heat and humidity fluxes between the vegetation and the overlying atmosphere as well as the mean wind speed within the canopy is improved by including the effects of atmospheric stability. Furthermore, two conservative flux conditions for heat and moisture in the vegetation layer are used, thus permitting a diagnostic calculation of the lower boundary condition for temperature and specific humidity of the atmospheric model, in agreement with Dickinson.

A new method is introduced by treating the three balance equations for the energy and moisture transfer at the ground surface and the energy state of the vegetation layer as a coupled system in the three independent variables T_f (foliage temperature), T_g (ground surface temperature) and q_g (ground surface specific humidity). This system is solved simultanously by an iterative procedure. The application of this technique together with the multilayer soil model should result in more realistic modeling of the atmospheric lower boundary conditions.

2. Model Description

2.1. The atmospheric model

The one-dimensional prognostic model comprises the horizontal motion u, v, the potential temperature θ and the specific humidity q.

$$\begin{aligned}
\frac{\partial u}{\partial t} &= \frac{\partial}{\partial z}\left(K_m \frac{\partial u}{\partial z}\right) + f(v - v_g)\,, \\
\frac{\partial v}{\partial t} &= \frac{\partial}{\partial z}\left(K_m \frac{\partial v}{\partial z}\right) - f(u - u_g)\,, \\
\frac{\partial \theta}{\partial t} &= \frac{\partial}{\partial z}\left(K_h \frac{\partial \theta}{\partial z}\right) - \left(\frac{p_0}{p}\right)^{R_0/c_p} \frac{1}{c_p \rho} \frac{\partial F_n}{\partial z}\,, \\
\frac{\partial q}{\partial t} &= \frac{\partial}{\partial z}\left(K_q \frac{\partial q}{\partial z}\right);
\end{aligned} \tag{1}$$

F_n is the net flux of radiation and f the Coriolis parameter. The notation is standard. For the calculation of the exchange coefficients of momentum, heat and moisture, K_m, $K_h = K_q$, the 2.5 closure model of Mellor and Yamada (1982) is used.

2.2. The soil model

The mean state of the physical variables is formulated for the calculation of heat and moisture fluxes from thermodynamic considerations. This requires the introduction of a suitable potential from which the gross properties regulating the flow can be determined.

2.2.1. *The Theory of the Soil System*

The soil model is based on the investigation of Sievers *et al.* (SFZ, 1983) who treat the soil as a porous medium consisting of the mass components M^k: dry air ($k = 0$), water vapor ($k = 1$) and liquid water ($k = 2$) in the pores of a soil matrix ($k = 3$). The same identification is used for other quantities whenever they occur. The matrix is assumed to be rigid and incompressible, i.e., the volume of a soil element is strictly correlated to the partial mass M^3 by $V = M^3/\rho^3$.

To proceed with the analysis, it is necessary to introduce the volumetric water vapor (η^1) and liquid water contents (η^2) defined by

$$\eta^1 = \frac{\rho^1}{\rho_2}, \qquad \eta^2 = \frac{\rho^2}{\rho_2}, \tag{2}$$

where ρ_2 is the density of bulk water and ρ^1, ρ^2 are the partial densities ($\rho^k = M^k/V$) of vapor and liquid water within the soil.

Suitable quantities for the thermodynamic description of the macroscopic soil state are the total energy E, the geopotential Φ, the partial masses M^k and the temperature T. In contrast to SFZ, where the enthalpy concept is used, pressure is not taken as an independent variable because of its strong variability particularly within water films. The present development replaces enthalpy by the more suitable internal energy U which is introduced by the definition

$$U = E - \sum_{k=0}^{k=3} M^k \Phi.$$

The quantity U contains both the microphysical internal energies of the soil components as well as the effects of adhesion and surface tension. These effects can be described either in terms of the internal energy U

$$U = \tilde{U} - \rho_2 V \int_0^{\eta^2} W(T, \xi)\, \mathrm{d}\xi\,, \tag{3}$$

or the free energy F

$$F = \tilde{F} + \rho_2 V \int_0^{\eta^2} \psi(T, \xi)\, \mathrm{d}\xi\,, \tag{4}$$

where the symbol (˜) denotes the (fictitious) internal and free energy without the adhesion effects. $W(T, \eta^2)$ is the differential heat of wetting and $\psi(T, \eta^2)$ the soil moisture potential. The application of the Helmholtz equation

$$U = F - T\left(\frac{\partial F}{\partial T}\right)_{M^k},$$

to (3) and (4) results in the known relation for the differential heat of wetting,

$$W(T, \eta^2) = -\psi(T, \eta^2) + T\left(\frac{\partial \psi}{\partial T}\right)_{\eta^2}. \tag{5}$$

The chemical potentials μ_k of the components $k = 0, 1, 2$ are related to the free energy by

$$\mu_k = \left(\frac{\partial F}{\partial M^k}\right)_{T,V,M^{i\neq k}}, \qquad k = 0, 1, 2\,. \tag{6}$$

The use of Equations (4) and (6) results in

$$\mu_0 = \tilde{\mu}_0, \qquad \mu_1 = \tilde{\mu}_1, \qquad \mu_2 = \tilde{\mu}_2 + \psi\,. \tag{7}$$

Chemical equilibrium will be assumed within the soil matrix, i.e., $\mu_1 = \mu_2$.

2.2.2. *The Prognostic Equations*

The development of the heat equation is based on the formulation of the internal energy and on the assumption of chemical equilibrium. This assumption implies that the partial densities ρ^1, ρ^2 as well as η^1, η^2 are no longer independent variables. From the total volumetric moisture content $\eta = \eta^1 + \eta^2$, one obtains functional relations of the form $\eta^1 = \eta^1(\eta, T)$, $\eta^2 = \eta^2(\eta, T)$. Therefore, the density of the internal energy $U/V = \rho e$, where e is the specific internal energy and ρ the total density, may be expressed as

$$\begin{aligned}\rho e = \rho e(T, \rho^0, \rho^1, \rho^2, \rho^3) &= \rho e(T, \rho^0, \eta^1, \eta^2, \rho^3) \\ &= \rho e(T, \rho^0, \eta, \rho^3)\,.\end{aligned}$$

The application of the partial time derivative to ρe yields

$$\frac{\partial \rho e}{\partial t} = \left(\frac{\partial \rho e}{\partial T}\right)_{\rho^0,\eta,\rho^3} \frac{\partial T}{\partial t} + \left(\frac{\partial \rho e}{\partial \rho^0}\right)_{T,\eta,\rho^3} \frac{\partial \rho^0}{\partial t} + \left(\frac{\partial \rho e}{\partial \eta}\right)_{T,\rho^0,\rho^3} \frac{\partial \eta}{\partial t}, \tag{8}$$

since $\partial\rho^3/\partial t$ vanishes. The partial internal energies for dry air M^0 and total water $M^W = M^1 + M^2$ are defined by

$$e_0 = \left(\frac{\partial U}{\partial M^0}\right)_{T,M^W,M^3} = \left(\frac{\partial \rho e}{\partial \rho^0}\right)_{T,\eta,\rho^3},$$
$$e_w = \left(\frac{\partial U}{\partial M^W}\right)_{T,M^0,M^3} = \frac{1}{\rho_2}\left(\frac{\partial \rho e}{\partial \eta}\right)_{T,\rho^0,\rho^3}. \tag{9}$$

The heat capacity for the soil by constant volume is given as

$$C_v = \frac{1}{V}\left(\frac{\partial U}{\partial T}\right)_{V,M^0,M^W} = \left(\frac{\partial \rho e}{\partial T}\right)_{\rho^3,\rho^0,\eta}. \tag{10}$$

With these abbreviations, Equation (8) becomes

$$\frac{\partial \rho e}{\partial t} = C_v \frac{\partial T}{\partial t} + e_0 \frac{\partial \rho^0}{\partial t} + e_w \rho_2 \frac{\partial \eta}{\partial t}. \tag{11}$$

Using Equation (3) with $\rho\tilde{e} = \tilde{e}_n \rho^n$ and (2) results in

$$\rho e = \frac{U}{V} = \rho^0 \tilde{e}_0 + \rho_2 \eta^1 \tilde{e}_1 + \rho_2 \eta^2 \tilde{e}_2 + \rho^3 \tilde{e}_3 - \\ - \rho_2 \int_0^{\eta^2} W(T, \xi)\, \mathrm{d}\xi. \tag{12}$$

From Equations (9) and (12) follows

$$e_0 = \tilde{e}_0, \qquad e_w = \tilde{e}_1 \frac{\partial \eta^1}{\partial \eta} + (\tilde{e}_2 - W)\frac{\partial \eta^2}{\partial \eta}. \tag{13}$$

To determine the time derivatives $\partial\rho^0/\partial t$, $\partial\eta/\partial t$ and $\partial\rho e/\partial t$ in (11), it is necessary to use budget equations. The quantity $\partial\rho^0/\partial t$ follows from the mass continuity equation for dry air

$$\frac{\partial \rho^0}{\partial t} + \nabla \cdot \mathbf{J}^0 = 0, \tag{14}$$

where $\mathbf{J}^0$ is the diffusion flux. The mass continuity equations for vapor and liquid water may be combined to give

$$\rho_2 \frac{\partial \eta}{\partial t} + \nabla \cdot (\mathbf{J}^1 + \mathbf{J}^2) = -S_\eta, \tag{15}$$

with the diffusion fluxes $\mathbf{J}^k (k = 1, 2)$. The sink $(-S_\eta)$ models the loss of moisture due to the soil-root system.

The budget equation for ρe is found from an extended analysis of SFZ (Equation (11)) where a source term S_e, corresponding to S_η has been added. This yields

$$\frac{\partial \rho e}{\partial t} + \nabla \cdot \mathbf{J}^Q = -\sum_{k=0}^{2} \mathbf{J}^k \cdot \nabla \Phi - S_e \,. \tag{16}$$

The vector $\mathbf{J}^Q$ denotes the heat flux in the soil system which is taken from SFZ (Equation (65)).

$$\mathbf{J}^Q = \mathbf{J}_i^Q + h_0 \mathbf{J}^0 + h_1 \mathbf{J}^1 + (\tilde{h}_2 + \psi)\mathbf{J}^2 \,, \tag{17}$$

where $h_0, h_1, \tilde{h}_2 + \psi$ are the enthalpies for dry air, water vapor and the soil liquid water, respectively. $\mathbf{J}_i^Q$ is the heat conduction flux which is proportional to $-\nabla T$.

The source term S_η in the mass budget equation (15) corresponds to the liquid water transport from the soil to the root system. Likewise, S_e in the heat budget Equation (16) corresponds to the heat transport coupled to this mass transport. Thus it seems reasonable to relate the source terms by analogy

$$S_e = (\tilde{h}_2 + \psi) S_\eta \,. \tag{18}$$

An expression for S_η is given later. Inserting (14), (15) and (16) in (11) together with relations (17), (18), one obtains the prognostic equation of temperature, i.e.,

$$\begin{aligned} C_v \frac{\partial T}{\partial t} &+ \nabla \cdot \{\mathbf{J}_i^Q + (h_0 - e_0)\mathbf{J}^0 + (h_1 - e_w)\mathbf{J}^1 \\ &+ (\tilde{h}_2 + \psi - e_w)\mathbf{J}^2\} = -(\tilde{h}_2 + \psi - e_w) S_\eta \\ &- \sum_{k=0}^{2} \mathbf{J}^k \cdot \nabla \Phi - \mathbf{J}^0 \cdot \nabla e_0 - (\mathbf{J}^1 + \mathbf{J}^2) \cdot \nabla e_w \,. \end{aligned} \tag{19}$$

The budget equations for dry air (14) and soil moisture (15) together with (19) now form a complete system of prognostic equations for the soil.

2.2.3. *Simplifications*

The solution of the three prognostic soil equations requires some simplifying assumptions. First of all, horizontal homogeneity is assumed. In comparison with the other terms in the temperature Equation (19), the influence of dry air as well as the change of potential energy into heat are neglected. Thus the prognostic equations reduce to

$$\frac{\partial \rho^0}{\partial t} + \frac{\partial J^0}{\partial z} = 0 \,,$$

$$\rho_2 \frac{\partial \eta}{\partial t} + \frac{\partial}{\partial z}(J^1 + J^2) = -S_\eta ,$$

$$C_v \frac{\partial T}{\partial t} + \frac{\partial}{\partial z}\{J_i^Q + (h_1 - e_w)J^1 + (\tilde{h}_2 + \psi - e_w)J^2\} = \tag{20}$$

$$-(\tilde{h}_2 + \psi - e_w)S_\eta - (J^1 + J^2)\frac{\partial e_w}{\partial z} ,$$

with $J^k = \mathbf{k} \cdot \mathbf{J}^k$ and $J_i^Q = \mathbf{k} \cdot \mathbf{J}_i^Q$.

The prognostic equation for temperature may be further simplified to

$$C_v \frac{\partial T}{\partial t} + \frac{\partial}{\partial z}(J_i^Q + (l_{21}(T) + W)J^1) = 0 , \tag{21}$$

in agreement with Philip (1957). The replacement of $(h_1 - e_w)$ by $(l_{21}(T) + W)$ is justified in Appendix A.1. Detailed numerical tests have shown that the neglected terms are several orders of magnitude smaller than the remaining terms. However, the flux J^1 in the prognostic equations for temperature and soil moisture has been retained. Model calculations (not discussed later) have revealed that in case of very low moisture content, the inclusion of J^1 is responsible for a temperature decrease of approximately 1 deg. There might be situations where the effect of this flux is even larger. Moreover, the inclusion of J^1 results in a more reasonable temperature and moisture distribution in the case of dry soil.

2.2.4. *Parameterization by Empirical Laws*

The evaluation of the prognostic equations requires parameterization of the heat conduction and diffusion fluxes. Here the results of SFZ (Equation (41) and (46)) are applied again to give approximately

$$J^1 = \hat{J}^1 + \frac{\rho^1}{\rho^0} J^0 \quad \text{and} \quad \hat{J}^1 = -\frac{D^{\text{vap}}}{R_1 T}\frac{\partial p^1}{\partial z} , \tag{22}$$

where the diffusion flux of dry air J^0 will be determined in the following section. The quantities p^1 and R_1 are the partial pressure and gas constant for water vapor. The diffusion coefficient D^{vap} is used as reported by SFZ. The diffusion flux of liquid water is described by Darcy's law

$$J^2 = -\frac{K_\eta \rho_2}{g}\frac{\partial}{\partial z}(\psi + \Phi) , \tag{23}$$

where K_η in $\mathrm{m\,s^{-1}}$ is the (unsaturated) hydraulic conductivity. The moisture potential ψ and K_η are taken from Clapp and Hornberger (1978). The heat conduction flux J_i^Q and C_v are used as given in Pielke (1984). The quantity $\partial\psi/\partial T$ is taken from Philip (1957).

2.2.5. *The Diffusion Flux for Dry Air*

The computation of J^1 in Equation (22) requires the diffusion flux J^0, which is difficult to parameterize due to its dependence on the unknown size distribution of the soil pores. Therefore, J^0 will be described diagnostically. The filter condition $\partial(p^0 + p^1)/\partial t = 0$ is introduced (p^0 is the partial pressure of dry air), because one may realistically expect a pressure balance within the pores at any time.

From Equation (20), J^0 may be determined in terms of p^0 which is given by

$$\rho^0 = (\pi - \eta^2)\frac{p^0}{R_0 T}, \tag{24}$$

where π is the soil porosity and R_0 the dry air gas constant. A little reflection shows that the dependence of ρ^0 on p^0, η^2 and T may be transformed to $\rho^0 = \rho^0(\eta, T, p^0 + p^1)$. Now one obtains

$$\left(\frac{\partial \rho^0}{\partial t}\right)_{p^o+p^1} = \left(\frac{\partial \rho^0}{\partial T}\right)_{\eta,p^0+p^1}\frac{\partial T}{\partial t} + \left(\frac{\partial \rho^0}{\partial \eta}\right)_{T,p^0+p^1}\frac{\partial \eta}{\partial t} = -\frac{\partial J^0}{\partial z}, \tag{25}$$

where the derivatives of ρ^0 with respect to T and η are given in Appendix A.2.

Integration of (25) from a fixed lower boundary within the soil to a variable upper limit z finally gives $J^0(z)$.

2.2.6. *The Prognostic System for the Soil*

The concept of this soil model is based on the assumption of chemical equilibrium. Inserting (25) into the moisture budget Equation (20) and into the temperature Equation (21) together with (22) results in the following system of coupled differential equations

$$\begin{aligned}
&\left\{\rho_2 - \frac{\rho^1}{\rho^0}\left(\frac{\partial \rho^0}{\partial \eta}\right)_{T,p^0+p^1}\right\}\frac{\partial \eta}{\partial t} - \frac{\rho^1}{\rho^0}\left(\frac{\partial \rho^0}{\partial T}\right)_{\eta,p^0+p^1}\frac{\partial T}{\partial t} + \\
&+ J^0\frac{\partial}{\partial z}\left(\frac{\rho^1}{\rho^0}\right) + \frac{\partial}{\partial z}(\hat{J}^1 + J^2) = -S_\eta, \\
&\left\{C_v - (l_{21}(T) + W)\frac{\rho^1}{\rho^0}\left(\frac{\partial \rho^0}{\partial T}\right)_{\eta,p^0+p^1}\right\}\frac{\partial T}{\partial t} - \frac{\rho^1}{\rho^0}(l_{21}(T) + W) \times \\
&\times \left(\frac{\partial \rho^0}{\partial \eta}\right)_{T,p^0+p^1}\frac{\partial \eta}{\partial t} + \frac{\partial}{\partial z}(J_i^Q + (l_{21}(T) + W)\hat{J}^1) + \\
&+ J^0\frac{\partial}{\partial z}\left((l_{21}(T) + W)\frac{\rho^1}{\rho^0}\right) = 0
\end{aligned} \tag{26}$$

whose numerical evaluation will be described later.

2.2.7. *Water Transport by the Root System*

To complete the soil model, it is necessary to parameterize the uptake of water by the root system. The model is based on the assumption that the amount of water extracted from the roots is balanced by the transpiration from the plant system above the soil. According to Hillel (1980), this balance appears to be realistic since only 1% of the transported water is used by the plants during the growing season. The intensity of evaporation, as steered by the vegetation model to be described later, depends on the total surface area of the roots per unit volume and its vertical distribution. Moreover, the distribution of the soil water as well as the force of gravity have an important influence. The reason is that the extraction of water from deeper layers requires more energy against the force of gravity than from upper layers, so that in general, the upper layers will be exhausted first. The extraction is limited by a lower boundary of the soil moisture content known as the wilting point. When this point is reached, the uptake of water becomes impossible.

Thermodynamic reasoning indicates that the flow of soil water into the roots is controlled by the difference of the chemical potentials between the soil water and the root system. In analogy to Equation (7), using the thermodynamic identity

$$\mu_2 = \tilde{\mu}_2 + \psi = \mu_2^+(T) + \frac{p - p_r}{\rho_2} + \psi \tag{27}$$

(μ_2^+ depends only on T, p_r is the reference pressure), the chemical potential for the root system is defined as

$$\mu_2^{\text{root}} = \mu_2^+(T) + \frac{(p + p^{\text{osm}}) - (p_r + p_r^{\text{osm}})}{\rho_2} + \psi^{\text{root}}. \tag{28}$$

The osmotic pressure p^{osm} is expressed in terms of its reference pressure as

$$p^{\text{osm}}(z) = p_r^{\text{osm}} - \rho_2 g z, \qquad z \leqslant 0. \tag{29}$$

The flow of water into the plant system will continue as long as the soil water chemical potential exceeds that of the root system ($\mu_2 > \mu_2^{\text{root}}$), i.e.,

$$\psi + gz - \psi^{\text{root}} > 0, \qquad z \leqslant 0. \tag{30}$$

It seems realistic to assume that the major uptake of water by the roots takes place in a soil layer where the difference of the potentials has the maximum value. In practice, the numerical value of ψ^{root} as a function of height is not available so that the inequality (30) cannot be used directly to determine the maximum value of the potential difference. Therefore, it is assumed that ψ^{root} is a constant and the water uptake, as regulated by S_η, takes place in that soil layer where the sum $\psi + gz$ is largest.

2.3. The canopy model

The canopy is treated as a single vegetation layer of height h whose lower boundary is the ground. This layer consists of the canopy air and the foliage of the plants. Following Geiger (1961), Monteith (1973) and others, the foliage is characterized by negligible storage of heat energy. This implies that the heat equation of the foliage reduces to a flux balance equation to be discussed in Section 2.3.6. Furthermore, it appears reasonable to neglect heat and water vapor storage as well as the absorption of radiation within the canopy air. These assumptions result in continuity statements for sensible heat and humidity fluxes. The development of temperature, humidity and wind speed within the canopy is controlled by the physical processes in the overlying atmosphere and within the soil system.

The vegetation is modeled in terms of the shielding factor σ_f and the leaf area index L_A. The quantity σ_f represents the mean coverage of the foliage per unit area, and L_A is the ratio of the total one-side leaf area to the vertical projection of the horizontal cross-section of the plant. Additionally, the mean wind speed u_{af}, the temperature T_{af} and the specific humidity q_{af} of the *a*ir within the *f*oliage as well as the *f*oliage temperature T_f and the saturation specific humidity $q_s(T_f)$ are needed to describe the physical processes within the canopy.

Effectively, Deardorff (1978) treats the canopy problem by solving a prognostic equation for the ground surface temperature T_g together with the heat balance equation for the canopy to determine the foliage temperature T_f. Finally he calculates the air temperature in the foliage T_{af} as a weighted mean of T_g, T_f and the air temperature directly above the canopy. He obtains the weighting factors from numerical experiments. Similarly he proceeds with the computation of q_{af}.

Dickinson (1984) modified and improved Deardorff's approach and obtained T_{af} and q_{af} in a more realistic manner by solving continuity statements for the sensible heat and water vapor fluxes, thus eliminating the empirical determination of the weighting factors.

The present model uses a coupled system of three balance equations for the energy and moisture at the earth's surface and an energy statement for the canopy in the three independent variables T_g, T_f and $q_g = q(z = 0)$, which may be calculated in an accurate manner from an iterative procedure. The advantage of the present scheme is that now q_g can be calculated directly and there is no need to specify q_g as a function of T_g and of some moisture parameters that are difficult to determine.

In summary, the canopy model requires computation of all energy fluxes at the earth's surface and in the canopy as well as the evapotranspiration and condensation (dew) on the foliage. Following Deardorff (1978), the storage of liquid water within the canopy will be computed prognostically.

2.3.1. *The Heat and Humidity Fluxes above the Canopy*

Heat and humidity fluxes, $H_{c,a}$ and $E_{c,a}$ from the canopy to the overlying atmosphere are calculated from Clarke's (1970) external constant flux layer formulation

in the form given by Panhans and Schrodin (1980). By linearizing $\theta(z)$, their equations are

$$H_{c,a} = |\mathbf{v}_h(z_1)| c_{c,a} \rho c_p (T_{af} - T(z_1) - \gamma_d (z_1 - d)) ,$$
$$E_{c,a} = |\mathbf{v}_h(z_1)| c_{c,a} \rho (q_{af} - q(z_1)) , \tag{31}$$

where $\mathbf{v}_h(z_1)$ is the horizontal velocity at the first prognostic level z_1 which is located above the canopy. The transfer coefficient $c_{c,a}$ is defined in terms of the Clarke stability functions G^m_{CL} for momentum and G^h_{CL} for heat,

$$c_{c,a} = \frac{1}{G^m_{CL}\left(\frac{z_p}{z_{0,c}}, \frac{z_p}{\lambda_{CL}(z_p\, z_{0,c})}\right) G^h_{CL}\left(\frac{z_p}{z_{0,c}}, \frac{z_p}{\lambda_{CL}(z_p, z_{0,c})}\right)} . \tag{32}$$

The quantity $z_p = z_1 - d$ introduces the zero displacement d of vegetation height h. Following Pielke (1984), $d \approx 3/4h$ and the roughness height for the canopy is $z_{0,c} \approx 1/3(h - d)$. For definition of the external stability length λ_{CL}, see Panhans and Schrodin.

The form of Equation (31) indicates that the product $(|\mathbf{v}_h(z_1)| c_{c,a})^{-1}$ may be interpreted as a resistance $r_{c,a}$ in analogy to Ohm's law, i.e.,

$$r_{c,a} = \frac{G^m_{CL}\left(\frac{z_p}{z_{0,c}}, \frac{z_p}{\lambda_{CL}(z_p, z_{0,c})}\right) G^h_{CL}\left(\frac{z_p}{z_{o,c}}, \frac{z_p}{\lambda_{CL}(z_p, z_{0,c})}\right)}{|\mathbf{v}_h(z_1)|} . \tag{33}$$

2.3.2. *The Wind Speed within the Canopy*

For determination of heat and humidity fluxes, it is mandatory to specify the mean wind speed u_{af} within the canopy. Since the atmospheric wind speed model is reliable only above the canopy, u_{af} must be obtained in some other way. Vegetation cannot always be characterized as dense so that the shielding factor is $\sigma_f < 1$. Therefore, Deardorff uses a very simple parameterization to obtain u_{af} in terms of a weighted average of the wind speeds u^v_{af} in dense vegetation ($\sigma_f = 1$) and u^0_{af} in the absence of foliage ($\sigma_f = 0$), i.e.,

$$u_{af} = \sigma_f u^v_{af} + (1 - \sigma_f) u^0_{af} . \tag{34}$$

His approximation $u^v_{af} = 0.83 u_*$ will also be used in the present model. Deviating from Deardorff, u^0_{af} is calculated in terms of the Clarke function from

$$u^0_{af}(z = d) = u^0_* G^m_{CL}\left(\frac{d}{z_{0,g}}, \frac{d}{\lambda_{CL}(d, z_{0,g})}\right) \tag{35}$$

for a wind profile extending down to the roughness height of the ground $z_{0,g}$. The friction velocities u^* and u^0_* with and without foliage may be computed from

$$u_* = \frac{|\mathbf{v}_h(z_1)|}{G^m_{CL}\left(\frac{z_1 - d}{z_0}, \frac{z_1 - d}{\lambda_{CL}(z_1, z_0)}\right)}. \tag{36}$$

In the absence of foliage $d = 0$ and $z_0 = z_{0,g}$ so that equation (36) yields u^0_*. Using $z_0 = z_{0,c}$, one obtains u_* in the presence of foliage.

2.3.3. *The Net Radiation Fluxes*

Net shortwave radiation fluxes $F_{S,G}$ at the ground surface and $F_{S,C}$ of the canopy result from a simple energy budget, see, e.g., Taconet *et al.* (1986),

$$F_{S,C} = S_d(h)\sigma_f(1 - a_f)\left(1 + \frac{(1 - \sigma_f)a_g}{1 - a_f a_g \sigma_f}\right), \tag{37}$$

$$F_{S,G} = S_d(h)\frac{(1 - \sigma_f)(1 - a_g)}{1 - a_f a_g \sigma_f}, \tag{38}$$

where $S_d(h)$ is the incoming shortwave radiation at the top of the canopy. The quantities a_g and a_f denote the shortwave albedo of the earth's surface and the foliage, respectively. In contrast to Deardorff's expressions, these formulas consider the multiple reflection of shortwave radiation between the ground and the canopy.

In the longwave region, it seems realistic to set the emissivities of the ground and the foliage equal to one. A simple energy budget results in

$$F_{L,C} = \sigma_f(L_d(h) + \sigma T_g^4 - 2\sigma T_f^4), \tag{39}$$

$$F_{L,G} = (1 - \sigma_f)L_d(h) + \sigma_f \sigma T_g^4 - \sigma T_f^4, \tag{40}$$

with $L_d(h)$ the incoming longwave radiation flux at the top of the canopy and σ the Stefan-Boltzmann constant. The quantities $S_d(h)$ and $L_d(h)$ may be calculated either by a fairly detailed two-stream approximation or by some empirical formula, e.g., Zdunkowski *et al.* (1982, 1975a and 1975b).

2.3.4. *The Heat and Humidity Fluxes from the Leaves*

Following Deardorff, the sensible heat and humidity exchange, H and E, between the leaves and the surrounding air are parameterized as

$$\begin{aligned} H &= 1.1\sigma_f L_A u_{af} c_{f,c} c_p \rho (T_f - T_{af}) \\ E &= \sigma_f L_A u_{af} c_{f,c} \rho (q_s(T_f) - q_{af}) r'' . \end{aligned} \tag{41}$$

Here $q_s(T_f)$ is the saturation value of the specific humidity at T_f; the factor 1.1 accounts for the effects of stems, twigs etc. which exchange heat but do not transpire. The transfer coefficient $c_{f,c}$ is parameterized as

$$c_{f,c} = 0.01\left\{1 + \frac{0.3\,\mathrm{m\,s^{-1}}}{u_{af}}\right\}. \tag{42}$$

The humidity flux E takes into account the effects of transpiration and evaporation of dew so that $E = \sigma_f L_A(E^t_{\mathrm{leaf}} + E^e_{\mathrm{leaf}})$ with the transpiration term

$$E^t_{\mathrm{leaf}} = \begin{cases} \dfrac{\rho}{r_a + r_s}\left(1 - \left(\dfrac{W_{\mathrm{dew}}}{W_{\mathrm{dmax}}}\right)^{2/3}\right)(q_s(T_f) - q_{af}) & \text{if } q_{af} \leqslant q_s(T_f) \\ 0 & \text{if } q_{af} > q_s(T_f)\,, \end{cases} \tag{43}$$

and the evaporation or condensation term

$$E^e_{\mathrm{leaf}} = \frac{\rho}{r_a}\begin{cases} \left(\dfrac{W_{\mathrm{dew}}}{W_{\mathrm{dmax}}}\right)^{2/3}(q_s(T_f) - q_{af}) & \text{if } q_{af} \leqslant q_s(T_f) \\ (q_s(T_f) - q_{af}) & \text{if } q_{af} > q_s(T_f)\,. \end{cases} \tag{44}$$

For further details, see Monteith (1973) and Deardorff. The parameter r'' appearing in (41) is formulated in terms of the generalized stomatal resistance r_s and the atmospheric resistance r_a, i.e.,

$$r'' = 1 - \frac{\delta_c r_s}{r_a + r_s}\left\{1 - \left(\frac{W_{\mathrm{dew}}}{W_{\mathrm{dmax}}}\right)^{2/3}\right\}. \tag{45}$$

In the case of condensation, $\delta_c = 0$, otherwise $\delta_c = 1$. The generalized stomatal resistance is taken from Pielke (1984),

$$r_s = r_c\left\{\frac{S_{\mathrm{d,max}}}{0.03S_{\mathrm{d,max}} + S_d(h)} + P + \left(\frac{\eta_{\mathrm{wilt}}}{\eta_{\mathrm{root}}}\right)^2\right\}, \tag{46}$$

where the minimum stomatal resistance r_c and the wilting moisture content η_{wilt} are listed for several plant and soil types. The moisture content of the root zone η_{root} is provided by the soil model. $S_{\mathrm{d,max}}$ is the maximum (noon) incoming solar radiation and P is a function of the time of year with $P = 0$ during the growing season.

The atmospheric resistance is parameterized as

$$r_a = \frac{1}{c_f u_{af}}. \tag{47}$$

Finally the quantities W_{dew} and W_{dmax} in (45) denote the mass of stored dew on the foliage per unit ground area with maximum value $W_{\mathrm{dmax}} \approx 0.2\,\mathrm{kg\,m^{-2}} \cdot \sigma_f L_A$.

The budget equation for W_{dew} is given by

$$\frac{\partial W_{\mathrm{dew}}}{\partial t} = -\sigma_f L_A E^e_{\mathrm{leaf}} + \sigma_f \mathrm{Pr}, \qquad 0 \leqslant W_{\mathrm{dew}} \leqslant W_{\mathrm{dmax}}\,, \tag{48}$$

where the precipitation flux Pr in ($\mathrm{kg\,m^{-2}\,s^{-1}}$) is formally included. If W_{dew} exceeds W_{dmax}, the difference is treated as a liquid water flux $-E^l_{g,c}$ from the foliage to the ground in the moisture balance of the earth's surface, i.e.,

$$E^l_{g,c} = -\frac{W_{\mathrm{dew}} - W_{\mathrm{dmax}}}{\Delta t} - (1 - \sigma_f)\mathrm{Pr}, \qquad W_{\mathrm{dew}} > W_{\mathrm{dmax}} \tag{49}$$

with Δt the integration time step.

In Section 2.2.7 it was mentioned that the loss of soil moisture due to the root system is balanced by the transpiration from the plant system. Therefore, the soil model is directly coupled to the canopy model since the sink term S_η is given by

$$S_\eta = \sigma_f L_A \frac{E^l_{\mathrm{leaf}}}{\Delta z_{\mathrm{root}}}, \tag{50}$$

where Δz_{root} is the thickness of the extraction layer of soil water due to the roots.

2.3.5. *Heat and Humidity Fluxes from the Ground to the Canopy*

In analogy to the flux formulation in (31), the heat and humidity fluxes from the ground to the canopy are formulated in terms of the transfer coefficient $c_{g,c}$,

$$\begin{aligned} H_{g,c} &= u_{af} c_{g,c} \rho c_p (T_g - T_{af} - \gamma_d d)\,, \\ E_{g,c} &= u_{af} c_{g,c} \rho (q_g - q_{af})\,, \end{aligned} \tag{51}$$

where $u_{af}c_{g,c}$ may be written as the reciprocal of the resistance $r_{g,c}$. This quantity accounts for both the aerodynamic resistance $r^0_{g,c}$ caused by the roughness of the ground surface and the additional resistance $r^f_{g,c}$ due to the drag exerted by the foliage, i.e.,

$$r_{g,c} = r^0_{g,c} + r^f_{g,c}\,. \tag{52}$$

The resistance $r^0_{g,c}$ is defined in analogy to $r_{c,a}$ in (33) as

$$r^0_{g,c} = \frac{G^m_{CL}\left(\dfrac{d}{z_{0,g}}, \dfrac{d}{\lambda_{CL}(d, z_{0,g})}\right) G^h_{CL}\left(\dfrac{d}{z_{0,g}}, \dfrac{d}{\lambda_{CL}(d, z_{0,g})}\right)}{u_{af}}, \tag{53}$$

but with respect to the velocity u_{af} coordinated to the zero displacement height d. The additional resistance $r^f_{g,c}$, as derived in Appendix A.3, is given by

$$r^f_{g,c} = \frac{\exp(0.27 L_A) - 1}{1.35(0.27\kappa_f)^2 u_{af}}, \tag{54}$$

where $\kappa_f \approx 2.25$ may be thought of as a von Kármán constant for vegetation.

2.3.6. *The Determination of T_{af} and q_{af}*

The neglect of heat and water vapor storage within the canopy results in the continuity statements for heat and humidity fluxes, i.e.,

$$\begin{aligned} H_{g,c} + H &= H_{c,a}\,, \\ E_{g,c} + E &= E_{c,a}. \end{aligned} \tag{55}$$

Inserting the flux relations (31), (41) and (51) in Equation (55) yields

$$\begin{aligned} T_{af} &= \frac{|\mathbf{v}_h(z_1)|c_{c,a}(T(z_1) + \gamma_d(z_1 - d) + u_{af}c_{g,c}(T_g - \gamma_d d) + 1.1\sigma_f L_A u_{af} c_{f,c} T_f}{|\mathbf{v}_h(z_1)|c_{c,a} + u_{af}c_{g,c} + 1.1\sigma_f L_A u_{af} c_{f,c}}\,, \\ q_{af} &= \frac{|\mathbf{v}_h(z_1)|c_{c,a}q(z_1) + u_{af}c_{g,c}q_g + \sigma_f L_A u_{af} c_{f,c} r'' q_s(T_f)}{|\mathbf{v}_h(z_1)|c_{c,a} + u_{af}c_{g,c} + \sigma_f L_A u_{af} c_{f,c} r''}\,, \end{aligned} \tag{56}$$

which are the temperature and moisture boundary conditions required by the atmospheric model. Evaluation of Equation (56) requires knowledge of the quantities T_f, T_g and q_g which will be calculated from the energy balances of the canopy (EC) and the soil surface (EG) and the moisture balance at the soil surface (MG),

$$\begin{aligned} EC(T_g, T_f, q_g) &= F_{S,C} + F_{L,C} - H - l_{21}E = 0 \\ EG(T_g, T_f, q_g) &= F_{S,G} + F_{L,G} - H_{g,c} + J_i^Q + L(E_{g,c}^l - J^2) = 0 \\ MG(T_g, T_f, q_g) &= E_{g,c} + E_{g,c}^l - J^1 - J^2 = 0 \end{aligned} \tag{57}$$

with $L = l_{21} + W$. Mathematical expressions are available for all fluxes in Equation (57), where J_i^Q, J^1 and J^2 are described in Section 2.2.4. This coupled system may be solved simultaneously by an iterative procedure as outlined in Appendix A.4.

2.4. NUMERICAL ASPECTS

The height of the modeled atmosphere extends to 3000 m and to a soil depth of 1.5 m. A non-uniform vertical grid is used for both regions to provide a high resolution near the earth's surface. For the discretization of the atmospheric prognostic equations a fully implicit scheme has been used excepting the turbulent kinetic energy equation in the 2.5 closure model which is solved as described by Yamada and Mellor (1975). For the soil the Crank–Nicholson scheme has been chosen, a method of second-order accuracy in time and space.

Lower atmospheric boundary conditions T_{af} and q_{af} and upper boundary conditions T_g and q_g for the soil are provided by the canopy model. The remaining boundary conditions are specified as

$$\left.\begin{aligned} &(u, v) = (u_g, v_g) \\ &\frac{\partial \theta}{\partial z} = 0.0035\ \mathrm{K\ m^{-1}} \\ &\frac{\partial q}{\partial z} = \alpha q_{N-1} \end{aligned}\right\} \quad \text{at } z = 3000\ \mathrm{m}$$

and (u, v) equals zero at the displacement height d. The quantity q_{N-1} refers to the specific humidity one grid point below the upper boundary and α is calculated from Möller (1973, p. 140). At a depth of 1.5 m within the soil, temperature and moisture values are held fixed.

Finally, in order to run the complete model, the soil-vegetation code requires the following input parameters:

Height of vegetation:	h
Leaf area index:	L_A
Shielding factor:	σ_f
Minimum stomatal resistance:	r_c
Root depth:	z_{root}
Foliage albedo:	a_f
Ground albedo:	a_g
Ground roughness:	$z_{0,g}$

The soil type must be specified for the soil model so that the corresponding parameters can be extracted from Clapp and Hornberger (1978); see Section 2.2.4. All other quantities have been evaluated in previous sections.

3. Results

3.1. Verification of the model

A verification of the present model is attempted using some recent observations. Some experimental but by no means complete data sets could be derived from the HAPEX–MOBILHY experiment in southwestern France during 1985 and 1986, see, e.g., André *et al.* (1986), Noilhan and Planton (NP, 1989), Jacquemin and Noilhan (1990) and others.

For verification of the present model, a reproduction of measured energy balances over vegetated surfaces is carried out by using the estimated canopy and vegetation parameters of NP for the two observational sites, Lubbon 2 and Catelnau. Typical atmospheric temperature and humidity profiles for this region given by Pinty *et al.* (1989) for early morning mid-June are used to initialize the atmospheric model. These stations differ in soil type (sand and loam) but are characterized by the same type of vegetation (maize). Furthermore, the vegetation differs

TABLE I

Vegetation parameters for the HAPEX–MOBILHY simulation

Site	Vegetation	Soil	h (m)	L_A	σ_f	a_f	r_c ($s\,m^{-1}$)
Lubbon 2	Maize	Sand	1.20	2.00	0.80	0.18	200
Castelnau	Maize	Loam	0.24	0.30	0.40	0.25	40

in height, shielding factor and leaf area index. The required vegetation parameters are summarized in Table I. The calculations begin at 0600 LST using the given initial atmospheric data with clear sky conditions and the measured value of soil moisture. Since initial soil temperatures are not available, they are estimated from Geiger (1961). The wind profile is calculated from a geostrophic wind of $10\,m\,s^{-1}$ to approximate the observed wind speed near the ground.

The results, refering to the following day of integration time, are presented in Figure 1(b) and 2(b). The atmospheric turbidity has been adjusted to reproduce the observed solar net radiation fluxes at noon at the vegetated surface. Using the notation of *NP*, the net radiation (*RN*), latent heat (*LE*), sensible heat (*H*) and soil heat flux (*G*) are modeled as

$$\begin{aligned} RN &= F_{S,C} + F_{S,G} + F_{L,C} + F_{L,G} \\ LE &= l_{21} E_{c,a} \\ H &= H_{c,a} \\ G &= -(J_i^Q + LJ^1)\,. \end{aligned} \tag{58}$$

The comparison in both cases shows reasonable agreement between simulation and observation. Especially the ratio of the sensible heat to the latent heat flux and their phase displacement of maximum values is reproduced well. The partition of energy in latent and sensible heat is mainly affected by the magnitude of the minimum stomatal resistance r_c. This was pointed out earlier by Taconet *et al.* (1986) and others. The values for r_c are estimated from Tjernström (1989).

It will be noticed that in both cases, there is some deviation in the soil heat fluxes which may be caused by incomplete and estimated canopy and soil parameters. No attempt was made to adjust these parameters and the initial soil temperature distribution to force detailed agreement with the measurements since this would not serve any useful purpose.

An additional model verification was carried out using the recent data from the LOTREX-10E/HIBE88 field experiment in Germany (1988). The atmospheric energy fluxes derived from the measurements, using Equation (58), were provided by the research group of Prof. Fiedler (Karlsruhe). Figure 3(a) and 4(a) show the observed energy fluxes over a wheat and a sugar beet field for July 13.

The rather complete set of measurements including soil moisture and temperature distributions are used to calculate the required energy fluxes. The necessary

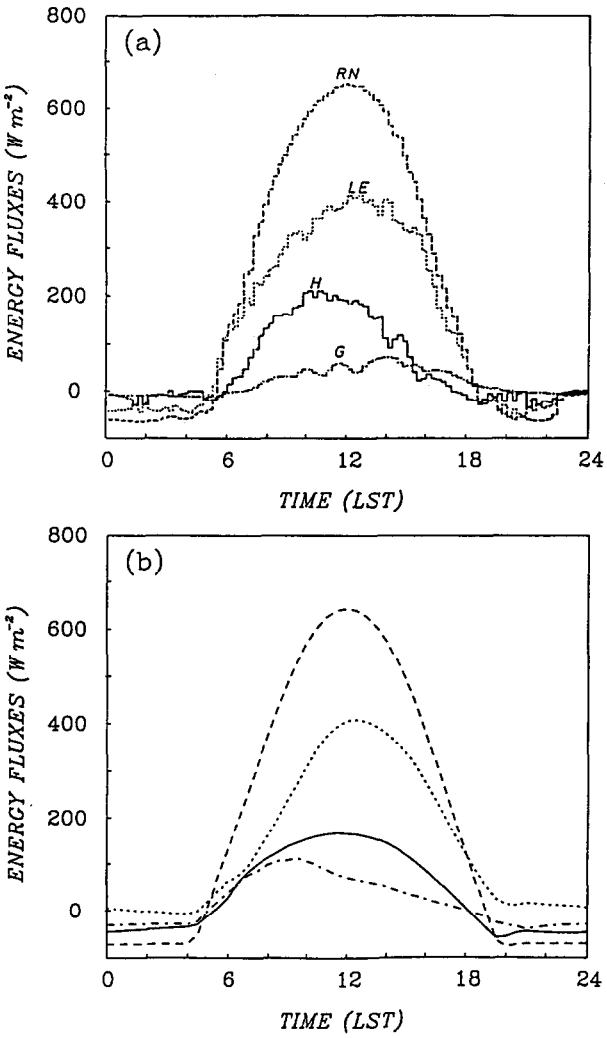

Fig. 1. Diurnal course of observed (a) and simulated (b) surface energy fluxes in ($W m^{-2}$) for the site *Lubbon 2*; the net radiation flux RN (dashed line), the latent heat flux LE (short dashed line), the sensible heat flux H (solid line) and the soil heat flux G (dash pointed line).

vegetation and soil parameters are taken from Schädler *et al.* (1990) and listed in Table II. The agreement between observed and calculated fluxes for both types of vegetation, as presented in Figure 3(b) and 4(b), is quite reasonable. As in the HAPEX–MOBILHY experiment, the calculated ratio of sensible to latent heat flux is reproduced fairly accurately. Moreover, their phase displacement is in good agreement with measurements.

As pointed out by the research group, some uncertainties are attached to the soil heat fluxes due to measurement difficulties. Furthermore, the calculated soil heat flux refers to the earth's surface while the observed flux pertains to a small

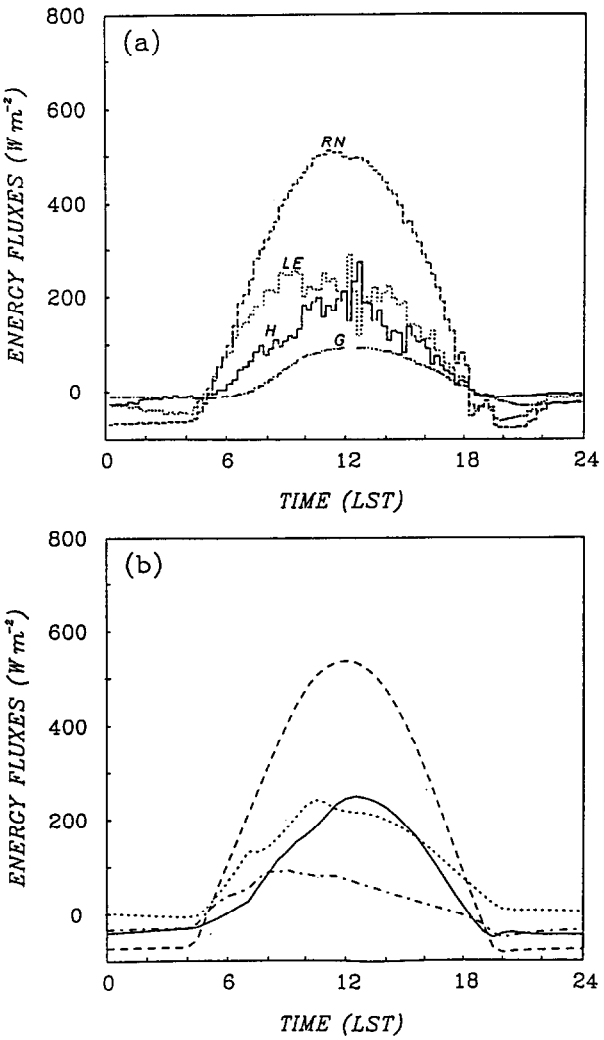

Fig. 2 . The same as in Figure 1 but for the site *Castelnau*.

distance within the soil. Therefore, it is not surprising that the measured energy fluxes are not completely balanced. This appears to explain the deviation of observation and theory.

3.2. Sensitivity studies

The comparison of observed and simulated surface energy fluxes indicates that the model works reasonable well. Now some numerical sensitivity studies are performed in order to investigate the influence of different soil and vegetation characteristics on the atmospheric energy state.

The calculations refer to a latitude of 50° N and a solar declination of 10°, as well as clear sky conditions and a moderately hazy atmosphere. The model is

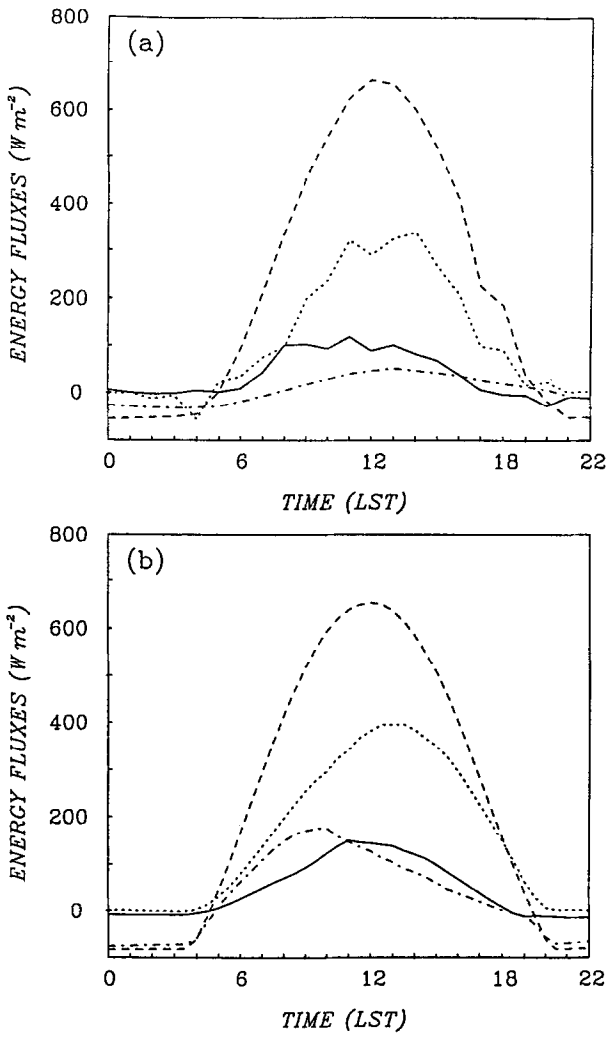

Fig. 3. Diurnal course of observed (a) and simulated (b) surface energy fluxes in (W m^{-2}) for a wheat field; the net radiation flux RN (dashed line), the latent heat flux LE (short dashed line), the sensible heat flux H (solid line) and the soil heat flux G (dash pointed line).

initialized with representative temperature and humidity profiles and a geostrophic wind of 4 m s^{-1}. The initial soil temperature distribution is derived from Geiger (1961). The numerical results refer to the second day of simulation; the model adjustment takes only a few hours.

3.2.1. *The Influence of the Shielding Factor*

The first test is a numerical experiment for a sunflower field with three different shielding factors ($\sigma_f = 0, 0.65, 0.95$). The soil type is sandy loam with a constant initial moisture distribution of $\eta = 0.15\ m^3\ m^{-3}$. The necessary canopy parameters

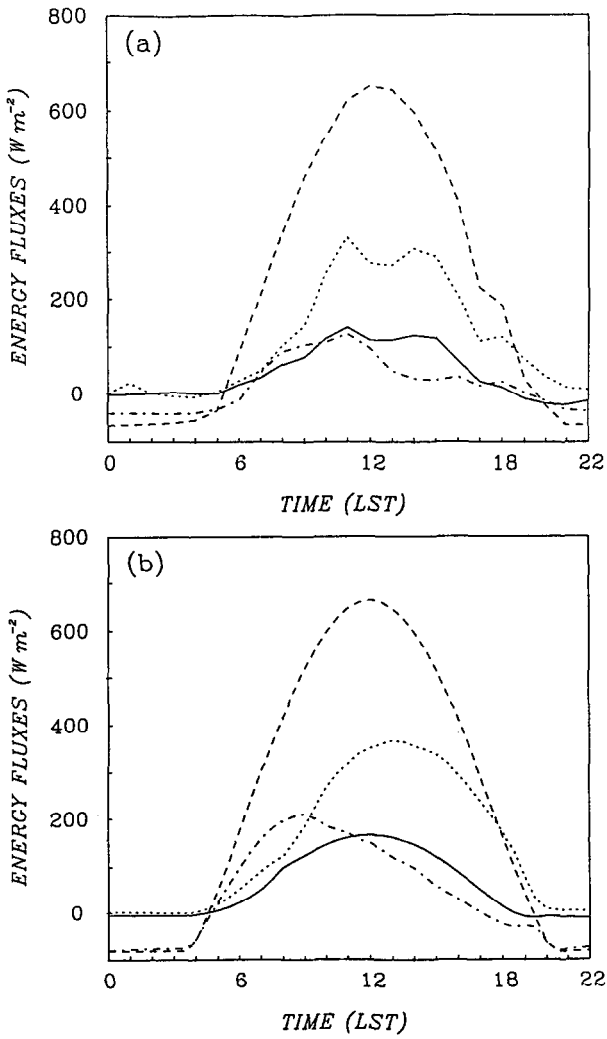

Fig. 4. The same as in Figure 3 but for a sugar beet field.

TABLE II

Vegetation parameters for the LOTREX-10E/HIBE88 simulation

Vegetation	Soil	h (m)	L_A	σ_f	a_f	r_c (s m^{-1})
Wheat	Sandy loam	0.88	5.3	0.70	0.20	300
Sugar beet	Sandy loam	0.24	2.2	0.45	0.20	250

as shown in Table III are derived from Pielke (1984). Figure 5 shows the atmospheric and the soil temperature distribution at noon and shortly before sunrise (0500 LST). At noon, the surface temperature ranges from 25 °C for bare soil to 20 °C for $\sigma_f = 0.95$. Even at a height of 100 m, an air temperature difference of

TABLE III

Vegetation parameters for a sunflower field

Vegetation type	Sunflower
Height of vegetation	1.50 m
Leaf area index	1.8
Minimum stomatal resistance	110 s m^{-1}
Root depth	1 m
Foliage albedo	0.20

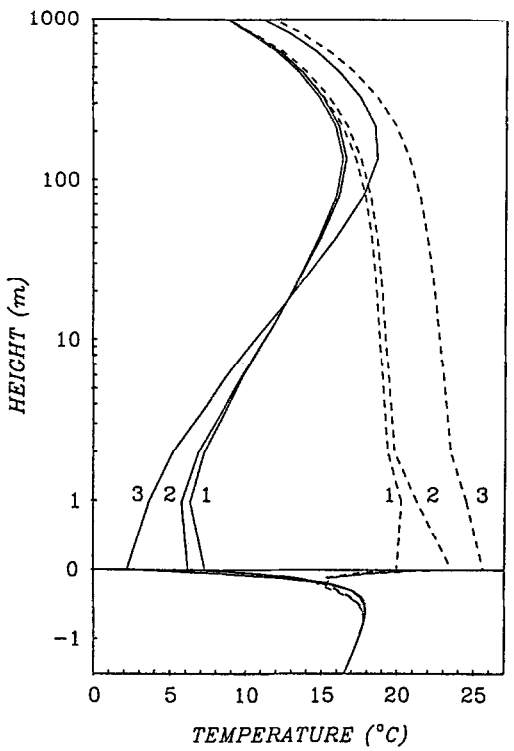

Fig. 5. The temperature profiles at 0500 LST (solid lines) and at 1200 LST (dashed lines) for the shielding factors $\sigma_f = 0.95$ (1), 0.65 (2) and 0 (3).

3 deg is obtained, showing the important effect of vegetation. The conditions are reversed in the morning hours.

Figure 6(a) shows the damping effect of the vegetation coverage on the amplitude of the daily temperature wave, which is most effective for high values of the shielding factor. Figure 6(b) depicts the specific humidity at the ground. The peculiar distribution – in agreement with Geiger (1961) – calls for some explanation. In the morning hours when vertical mixing is weak, an increase in specific humidity takes place until a maximum value is reached due to an accumulation of moisture resulting from the surface evaporation. After the ground inversion has dissipated, vertical mixing increases until a nearly uniform water vapor profile is

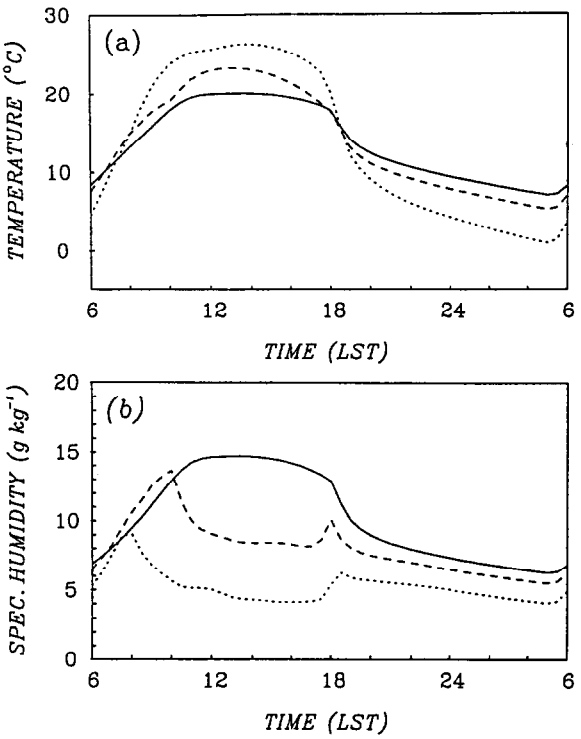

Fig. 6. The diurnal course of temperature (a) and the specific humidity (b) at the ground surface for the shielding factors $\sigma_f = 0.95$ (solid line), 0.65 (dashed line) and 0 (short dashed line).

formed within the mixing layer. In the case of $\sigma_f = 0$ and 0.65, this is accompanied by a decrease in specific humidity from the first maximum in the morning hours to a nearly constant value existing until 1800 LST. The development of a weak ground temperature inversion in the early evening leads to a second maximum whose intensity is limited by a decrease in evaporation due to insufficient solar energy.

Increasing vegetation coverage prevents the drying of the uppermost soil layers. Therefore, in the case of $\sigma_f = 0.95$, the moisture loss from the ground is reduced since the upward moisture transport is not as strong as for lower values of σ_f. Comparison of Figure 6(a) and 6(b) indicates that the daily run of the surface specific humidity in this case follows closely the temperature wave.

Figure 7 and 8 display contour plots of the diurnal course of the soil temperature (a) and the moisture content (b) for the shielding factors $\sigma_f = 0$ and 0.65. The distributions are plotted to a depth where no noticeable changes in time occurs. Note that the ordinate values are displayed as equidistant model levels within the soil.

The major result obtained is that in the case of bare soil, the uppermost soil layers are more strongly heated than for $\sigma_f = 0.65$ resulting in a stronger drying

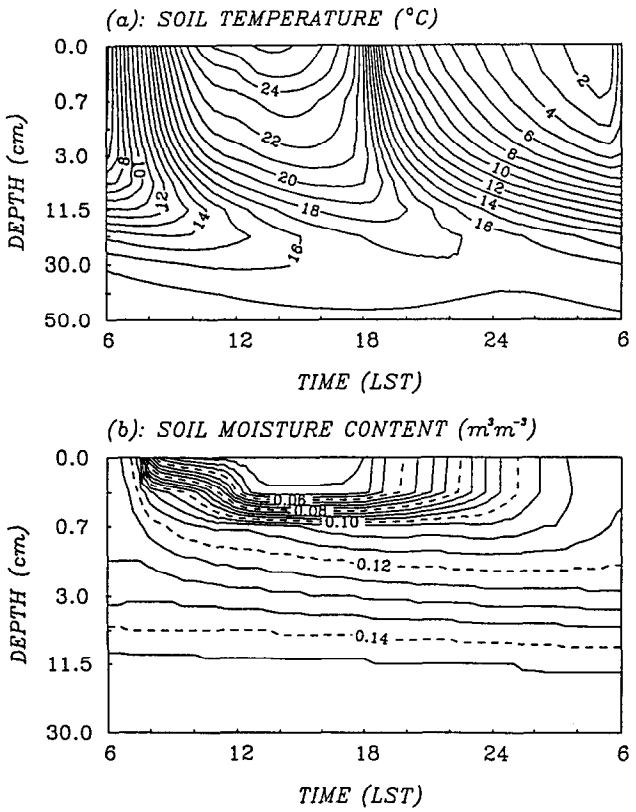

Fig. 7. Contour plots of the diurnal course of the soil temperature (a) and moisture distribution (b) for the shielding factor $\sigma_f = 0$.

effect for $\sigma_f = 0$. The penetration depth of the daily temperature wave is less than 50 cm, in agreement with Geiger, independent of σ_f.

3.2.2. *The Influence of Different Soil Moisture Contents*

In order to investigate the influence of soil moisture, additional calculations are performed for the same soil and vegetation type but using a different initial soil moisture content of $\eta = 0.26\ \mathrm{m^3\ m^{-3}}$.

Table IV presents the temperature differences between the simulations for the initial moisture content of $\eta = 0.15$ and 0.26 for two shielding factors. All other parameters remain the same. The results are displayed for the indicated shielding factors and times when approximately minimum and maximum temperatures occur. For both $\sigma_f = 0.65$ and 0.95, the largest temperature differences are found at 0500 LST. At noon, ΔT is relatively small except at $z = 0$. Inspection of Table IV shows the same qualitative behaviour of ΔT for the two shielding factors. The previously described damping effect of the larger vegetation cover is evident. Now the question arises if the variation in moisture content from $\eta = 0.15$ to $\eta = 0.26$ has a greater influence on ΔT than the range in vegetation cover from $\sigma_f = 0.65$

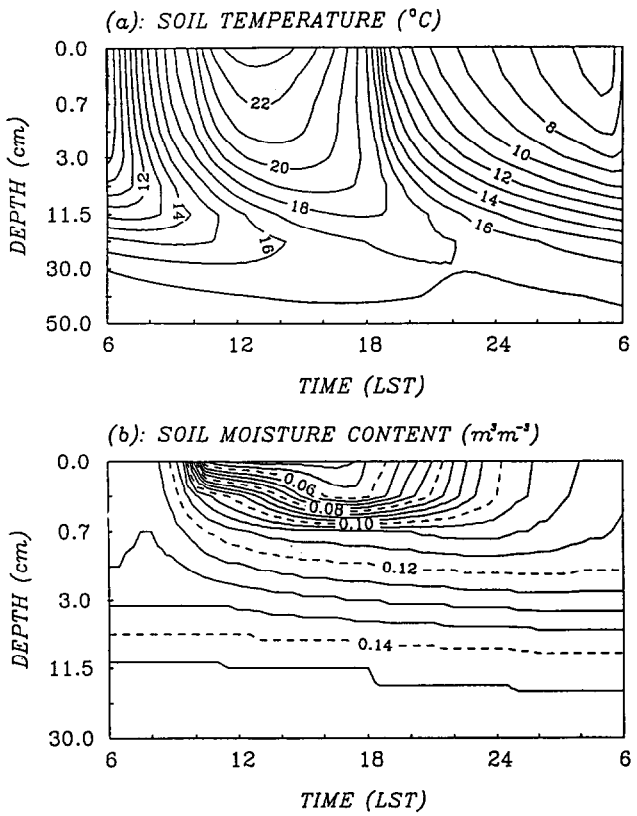

Fig. 8. The same as in Figure 7 but for the shielding factor $\sigma_f = 0.65$.

TABLE IV

Temperature differences $\Delta T = T(z, \eta = 0.15) - T(z, \eta = 0.26)$ at various heights, fixed local standard times (LST) and two shielding factors σ_f for a sunflower field. The zero displacement height is $d = 1.12$ m

	$\sigma_f = 0.65$		$\sigma_f = 0.95$	
z (m)	ΔT (5 LST)	ΔT (12 LST)	ΔT (5 LST)	ΔT (12 LST)
10.00	−1.6	0.5	−1.6	0.1
2.00	−3.6	0.6	−3.4	0.1
1.12	−4.1	0.9	−3.9	0.2
0.00	−4.6	3.8	−4.1	1.4
−0.03	−3.0	0.7	−2.9	0.5

to $\sigma_f = 0.95$ or vice versa. To answer this question, refer to Table V which displays temperature differences between the simulations for $\sigma_f = 0.65$ and 0.95 for various heights, fixed times and moisture content. Comparison of Tables IV and V shows that the influence of soil moisture is dominant particularly in the morning hours before sunrise. At this time, solar radiation is absent and wind and turbulent

TABLE V

Temperature differences $\Delta T = T(z, \sigma_f = 0.65) - T(z, \sigma_f = 0.95)$ at various heights, fixed local standard times (LST) and two initial soil moistures η for a sunflower field. The zero displacement height is $d = 1.12$ m

	$\eta = 0.15\ m^3\ m^{-3}$		$\eta = 0.26\ m^3\ m^{-3}$	
z (m)	ΔT (5 LST)	ΔT (12 LST)	ΔT (5 LST)	ΔT (12 LST)
10.00	0.0	0.4	−0.1	0.0
2.00	−0.4	0.4	−0.2	0.0
1.12	−0.5	0.7	−0.2	0.1
0.00	−1.1	3.4	−0.6	1.1
−0.03	−0.6	1.4	−0.5	1.1

TABLE VI

The characteristic parameters for sunflower, maize and prairie grass

Vegetation type	Sunflower	Maize	Grass
Leaf area index	3.6	4	2
Minimum stomatal resistance ($s\ m^{-1}$)	80	400	400

mixing near the ground are very weak so that the influence of the vegetation cannot be effective. Only during the noon hours at the earth's surface is the influence of vegetation comparable to the soil moisture effect. Particularly during the time of strong solar heating, the influence of increasing σ_f for a fixed initial value of η works in the same direction as the influence of increasing soil moisture η for fixed σ_f.

3.2.3. *The Influence of Different Vegetation Types*

Next we present a sensitivity study utilizing three vegetation types which are mainly characterized by the leaf area index and the minimum stomatal resistance. In all cases, the soil type is sandy loam. The initial soil moisture is assumed as $\eta = 0.17\ m^3\ m^{-3}$ at all depths. The vegetation is characterized by fields of sunflower, maize and prairie grass with $\sigma_f = 0.75$. For a better comparison of these three cases, uniform values of the vegetation height of 1.5 m, root depth of 0.90 m and foliage albedo of $a_f = 0.20$ are used. The characteristic canopy parameters, as shown in Table VI, are derived from Pielke (1984). The sunflower and maize fields strongly differ in the minimum stomatal resistance while the leaf area index is about the same. Maize and prairie grass have equal resistances but different leaf area indices.

Figure 9 displays the diurnal course of the energy fluxes for the sunflower (a) and maize field (b). The fluxes are defined by Equation (58). The most significant difference in computational results is the partition into the sensible and latent heat fluxes. While at noon the sensible and latent heat fluxes in the maize field are of

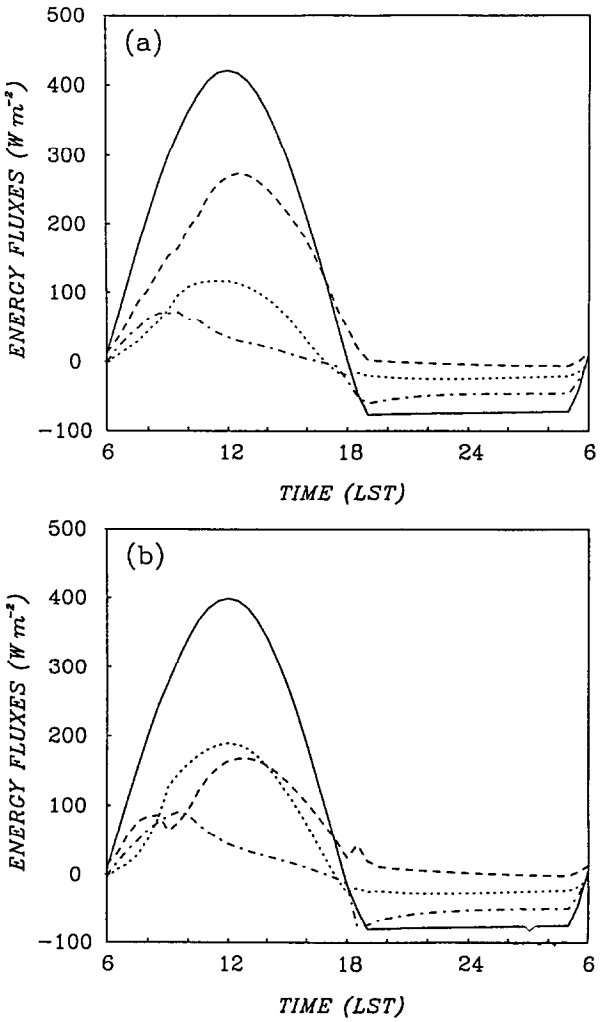

Fig. 9. Diurnal course of the surface energy fluxes in ($W\,m^{-2}$) for a sunflower (a) and a maize field (b); the net radiation flux RN (solid line), the latent heat flux LE (dashed line), the sensible heat flux H (short dashed line) and the soil heat flux G (dash pointed line).

about the same magnitude (Figure 9(b)), the latent heat flux is 2.3 times larger than the sensible heat flux in the case of sunflowers. The energy fluxes for prairie grass (not shown) are about as large as for the maize field although their leaf area indices differ by a factor of two. The different ratio of the latent and sensible heat fluxes results in different temperature and moisture distributions in the atmosphere. Some results are summarized in Table VII as differences of the maximum and minimum values of temperature and the specific humidity during a daily run at different heights.

Since the energy fluxes for maize and grass are nearly the same, no significant differences in the results are noticeable. A comparison of sunflower and maize

TABLE VII

The temperature and specific humidity differences between the maximum and minimum values of a diurnal course. The zero displacement height is $d = 1.12$ m for the three vegetation types

	$T_{max} - T_{min}$ (°)			$q_{max} - q_{min}$ (g kg^{-1})		
z (m)	Sunflower	Maize	Grass	Sunflower	Maize	Grass
10.00	7.2	8.5	8.1	1.9	1.9	1.8
2.00	11.6	13.7	13.2	3.2	2.5	2.3
1.12	13.3	16.0	15.4	4.0	3.5	2.9
0.00	12.1	14.1	14.0	7.9	9.2	9.2

shows that an increase of sensible heat flux and a decrease of latent heat flux, mainly forced by the minimum stomatal resistance, results in an increase in the temperature amplitude and in a decrease in humidity amplitude. An exception is the earth's surface where the difference of specific humidities is not so much controlled by evapotranspiration as by the surface temperature.

3.2.4. *The Influence of Precipitation*

In order to investigate the influence of precipitation, some calculations are performed assuming a precipitation rate of 2 cm in 2 h (Pr = 2.78 g m^{-2} s^{-1}) which is typical of a convective event in summertime. A cloud base was assumed at a height of 1.5 km. The rain occurs between 1400 and 1600 LST on the first day of the prediction period, accompanied by increasing cloud coverage one hour before the event, decreasing to zero coverage half an hour afterwards. The essential vegetation parameters are given in Table III using a shielding factor $\sigma_f = 0.6$. The soil type is sandy loam with an initial linear moisture distribution of $\eta = 0.13$ m^3 m^{-3} at the surface to 0.16 m^3 m^{-3} at a depth of 1 m.

Figure 10(a)–(d) shows the course of the surface temperature (T_g), the foliage temperature (T_f) the air temperature (T_{af}) within the foliage and the atmospheric temperature above the canopy (T_a) at $z = 2$ m from the first day of simulation at 0600 LST to the second day in the evening at 1800 LST. The solid lines refer to clear sky while the dashed lines represent the effect of cloudiness on temperature without any precipitation. The short dashed lines show the influence of rain.

The influence of cloud coverage on temperature is only noticeable during the time of cloud occurrence. In the case of precipitation, a decrease of temperature occurs resulting in a damping effect of the temperature wave for the remainder of the prediction time. A major part of the rain is stored within the soil, increasing the soil moisture and resulting in the effects described in Section 3.2.2. Inspection of Figure 10(a)–(d) shows that the influence of precipitation is very pronounced on the temperature pattern. The increased temperature T_g during the night due to increased heat capacity of the soil mainly drives the temperatures T_f, T_{af} and T_a. Furthermore, T_f is additionally influenced by the leaf storage of liquid water.

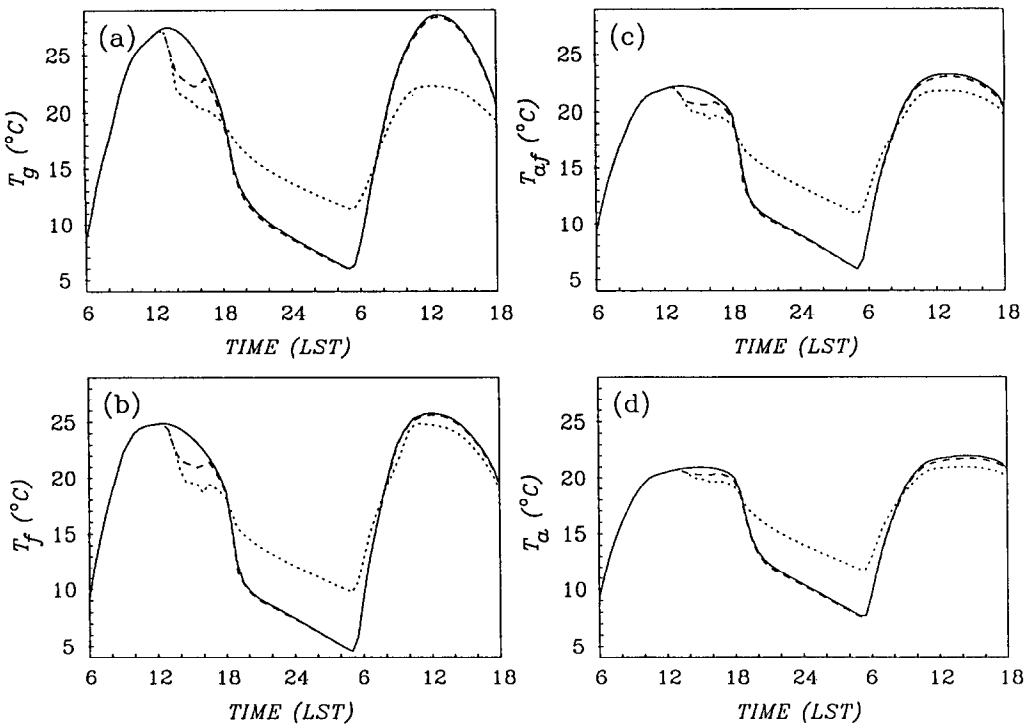

Fig. 10. The simulated course of the surface temperature (a), the foliage temperature (b), the air temperature within the foliage (c) and the atmospheric temperature above the canopy at $z = 2$ m (d); clear sky conditions (solid lines), cloudiness without precipitation (dashed lines), rainfall (short dashed lines).

During the second day the surface temperature T_g is strongly reduced because of the effective surface evaporation.

4. Summary and Conclusion

A one-dimensional soil-canopy model is introduced, which describes the influence of different soil and vegetation types on the energy state of the atmosphere. In contrast to other authors, the present canopy model uses a coupled system of three balance equations for the energy and moisture at the ground surface and the energy state of the canopy in three independent variables T_f (foliage temperature), T_g (ground surface temperature) and q_g (ground surface specific humidity), which are solved simultaneously. This procedure permits diagnostic calculation of the lower boundary conditions of temperature T_{af} and specific humidity q_{af} for the atmospheric model. Furthermore, the presented soil model, as derived from thermodynamic reasoning, provides a coupled system of two differential equations for soil temperature and moisture content.

For verification of this model, a comparison of calculated and observed energy

fluxes was presented for two sites of the HAPEX–MOBILHY experiment in southwestern France and the recent LOTREX-10E/HIBE88 field experiment in Germany. The model was found to be capable of simulating reasonably well the diurnal course of energy fluxes. In particular, the ratio of latent to sensible heat flux was properly simulated as well as the phase relation.

Finally, some sensitivity studies were performed in order to investigate the influence of different soil and vegetation parameters on the atmospheric energy state. The tests indicate

- the strong damping effect of increasing vegetation coverage on the daily temperature wave,
- prevention of the drying of the uppermost soil layers by increasing vegetation coverage,
- a stronger influence of soil moisture on the temperature than the shielding factor,
- the importance of the minimum stomatal resistance r_c since the ratio of latent to sensible heat energy is largely controlled by this quantity,
- the weak influence of the leaf area index on the atmospheric energy state in all inspected cases.

Moreover, the influence of a precipitation event during the prediction period on the course of T_g, T_f, T_{af} and T_a was shown. Additional sensitivity studies on various root depths for the discussed cases have been performed. Results are not presented because of their weak influence on the energy state of the atmosphere. The numerical effort of the soil-canopy model remains in reasonable bounds even though the soil model appears to be quite complicated. Therefore, the soil-canopy model is suitable for incorporation into a three-dimensional mesoscale prediction scheme.

Finally, the vegetation model has not been applied to extended canopies such as forests and orchards. However, the authors intend to generalize the single-layer scheme to a multilayer canopy. The problems associated with radiation transfer and turbulence, for example, are difficult to resolve but will be attacked in the near future.

A. Appendix

A.1. Latent heat of vaporization

The expression $(h_1 - e_w)$ in Equation (20) will now be simplified by using the realistic approximation $\partial\eta^2/\partial\eta = 1$. In this case, (13) reduces to

$$e_w = \tilde{e}_2 - W = \tilde{h}_2 - W - \frac{p}{\rho_2}, \tag{A1}$$

where the basic thermodynamic relation $\tilde{e}_2 = \tilde{h}_2 - p/\rho_2$ has been used. p is the total

pressure of the system which is approximated by the air pressure. The latent heat of vaporization for bulk water is defined as

$$l_{21}(T) = h_1 - \tilde{h}_2 , \tag{A2}$$

with $h_1 = \tilde{h}_1$ since $\mu_1 = \tilde{\mu_1}$, see (7). Combining (A1) and (A2) results in

$$h_1 - e_w = l_{21}(T) + W . \tag{A3}$$

The quantity p/ρ_2 was omitted since it is several orders of magnitude smaller than $l_{21}(T)$.

A.2. Derivation of ρ^0 with respect to T and η

Since $p^0 + p^1 = \text{const.}$ and $p^1 = p^1(\eta, T)$ the derivatives of ρ^0 are found to be

$$\left(\frac{\partial \rho^0}{\partial T}\right)_{\eta, p^0+p^1} = -\rho^0 \left\{ \frac{1}{\pi - \eta^2} \left(\frac{\partial \eta^2}{\partial T}\right)_\eta + \frac{1}{p^0} \left(\frac{\partial p^1}{\partial T}\right)_\eta + \frac{1}{T} \right\}, \tag{A4}$$

$$\left(\frac{\partial \rho^0}{\partial \eta}\right)_{T, p^0+p^1} = -\rho^0 \left\{ \frac{1}{\pi - \eta^2} \left(\frac{\partial \eta^2}{\partial \eta}\right)_T + \frac{1}{p^0} \left(\frac{\partial p^1}{\partial \eta}\right)_T \right\}, \tag{A5}$$

where p^1 is given by Edlefsen and Anderson (1943).

A.3. The resistance $r^f_{g,c}$

The Lovett wind profile, referenced in various papers, for the vegetation canopy apparently is of empirical nature and has probably been derived from measurements. It is defined by

$$u(z) = u(h) \exp(-0.27 CL_A(z)) \quad \text{with } h := \text{the vegetation height} , \tag{A6}$$

where the cumulative leaf area index CL_A is given by

$$CL_A(z) = \int_z^h \rho_l(z')\, \mathrm{d}z' . \tag{A7}$$

If $z = 0$ then $CL_A(z = 0)$ is the leaf area index L_A. Equation (A6) satisfies the steady state horizontal equation of motion considering only turbulent exchange and drag by the vegetation, i.e.,

$$\frac{\partial}{\partial z}\left(K_m \frac{\partial u}{\partial z}\right) - c_d \rho_l(z) u(z) |u(z)| = 0 , \tag{A8}$$

with a drag coefficient $c_d \approx 0.2$ for vegetation and ρ_l the leaf area density. If the exchange coefficient in Equation (A8) is given by the constant flux layer formulation,

$$K_m = l^2(z) \left| \frac{\partial u}{\partial z} \right| , \tag{A9}$$

then the mixing length is identified by

$$l(z) = \frac{2.25}{\rho_t(z)} . \tag{A10}$$

The quantity $\kappa_f = 2.25$ may be thought of as a von Kármán constant for vegetation. The integration of the steady state condition for the specific humidity

$$\frac{\partial}{\partial z}\left(K_h \frac{\partial q}{\partial z} \right) = 0 . \tag{A11}$$

with $K_h \approx 1.35 K_m$ yields the humidity flux

$$E_{g,c} \approx -\rho K_h \frac{\partial q}{\partial z} \approx -1.35\rho \frac{(0.27\kappa_f)^2 u_{af}}{\exp(0.27 L_A) - 1} (q_{af} - q_g) , \tag{A12}$$

where $(q(h) - q_g)$ is approximated by $(q_{af} - q_g)$ with $q_{af} = q(z = d)$. The analogy to (A12) with Ohm's law results in the resistance

$$r^f_{g,c} = \frac{\exp(0.27 L_A) - 1}{1.35(0.27\kappa_f)^2 u_{af}} . \tag{A13}$$

A.4. The numerical solution of the balance equations

For the numerical solution of the balance equations in (57), the Newton–Raphson method for a system of equations is used, i.e.,

$$\mathbf{x}^{i+1} = \mathbf{x}^i - (\mathbf{Df}(\mathbf{x}^i))^{-1} \cdot \mathbf{f}(\mathbf{x}^i); \qquad i = 0(1)n . \tag{A14}$$

with

$$\mathbf{x} = (T_f, T_g, q_g)^T, \qquad \mathbf{f}(\mathbf{x}) = (EC, EG, MG)^T \tag{A15}$$

and the functional matrix

$$\mathbf{Df}(\mathbf{x}) = \begin{pmatrix} \frac{\partial EC}{\partial T_f} & \frac{\partial EC}{\partial T_g} & \frac{\partial EC}{\partial q_g} \\ \frac{\partial EG}{\partial T_f} & \frac{\partial EG}{\partial T_g} & \frac{\partial EG}{\partial q_g} \\ \frac{\partial MG}{\partial T_f} & \frac{\partial MG}{\partial T_g} & \frac{\partial MG}{\partial q_g} \end{pmatrix} \tag{A16}$$

Acknowledgment

Gratitude is expressed to the computer center of the University of Mainz for providing computer time and to Prof. F. Fiedler for providing experimental data of the LOTREX-10E/HIBE88 field experiment.

References

André, J. C., Goutorbe, J. P., and Perrier, A.: 1986, 'HAPEX-MOBILY: A Hydrologic Atmospheric Experiment for the Study of Water Budget and Evaporation Flux at the Climate Scale', *Bull. Amer. Meteorol. Soc.* **67**, 138–144.

Clapp, R. and Hornberger G.: 1978, 'Empirical Equations for Some Soil Hydraulic Properties', *Water Resour. Res.* **14**, 601–604.

Crowan, I. R.: 1968, 'Mass Heat and Momentum Exchange between Stands of Plants and Their Atmospheric Environments', *Ibid.* **94**, 523–544.

Deardorff, J. W.: 1978, 'Efficient Prediction of Ground Surface Temperature and Moisture, with Inclusion of a Layer of Vegetation', *J. Geophy. Res.* **83**, 1889–1903.

Dickinson, R. E.: 1984, 'Modeling Evapotranspiration for Three-Dimensional Global Climate Models', in J. E. Hanson and T. Takahasi (eds.), *Climate Processes and Climate Sensitivity*, Amer. Geophys. Union, *Geophy Monogr.* **29**, 58–72.

Edlefsen, N. E. and Anderson, A. B. C.: 1943, 'Thermodynamics of Soil Moisture', *Hilgardia* **15**, 31–298.

Geiger, R.: 1961, *Das Klima der bodennahen Luftschicht*, Friedr. Vieweg & Sohn, Braunschweig, 646 pp.

Hillel, D.: 1980, *Fundamentals of Soil Physics*, Academic Press, New York, 413 pp.

Hillel, D.: 1980, *Application of Soil Physics*, Academic Press, New York, 385 pp.

Jacquemin, G. and Noilhan, J.: 1990, 'Sensitivity Study and Validation of a Land Surface Parameterization Using the HAPEX–MOBILHY Data Set', *Boundary-Layer Meteorol.* **52**, 93–134.

McCumber, M. C. and Pielke, R. A.: 1981, 'Simulation of the Effects of Surface Fluxes of Heat and Moisture in a Mesoscale Numerical Model. Part I: Soil Layer', *J. Geophys. Res.* **86**, 9929–9938.

Mellor, G. L. and Yamada T.: 1982, 'Development of a Turbulence Closure Model for Geophysical Fluid Problems', *Rev. Geophy. Space Phys.* **20**(4), 851–875.

Möller, F.: 1973, *Einführung in die Meteorologie Band I*, BI-Hochschultaschenbücher, Mannheim, 222 pp.

Monteith, J. L.: 1984, *Principles of Environmental Physics*, Edward Arnold, London, 241 pp.

Monteith, J. L.: 1975, *Vegetation and the Atmophere. Vol. 1: Principles*. Academic Press, 278 pp.

Noilhan, J. and Planton, S.: 1989, 'A Simple Parameterization of Land Surface Processes for Meteorological Models', *Monthly Weather Rev.* **117**, 536–549.

Panhans, W.-G. and Schrodin, R.: 1980, 'A One-Dimensional Circulation and Climate Model and its Application to the Lower Atmosphere', *Beitr. Phys. Atmoph.* **53**, 264–294.

Philip, J. R.: 1957, 'Evaporation and Moisture and Heat Fields in the Soil', *Journ. Met.* **14**, 354–366.

Philip, J. R. and De Vries, D. A.: 1957, 'Moisture Movement in Porous Materials under Temperature Gradients', *Trans. Amer. Geophy. Union* **38**, 222–232.

Pielke, R. A.: 1984, *Mesoscale Meteorological Modeling*, Academic Press, New York, 612 pp.

Pinty, J. P., Mascart, P., Richard, E., and Rosset, R.: 1989, 'An Investigation of Mesoscale Flows Induced by Vegetation Inhomogeneities Using an Evapotranspiration Model Calibrated Against HAPEX–MOILHY Data', *J. Appl. Meteorol.* **28**, 976–992.

Schädler, G., Kalthoff, N., and Fiedler, F.: 1990, 'Validation of a Model for Heat, Mass and Momentum Exchange over Vegetated Surfaces Using LOTREX-10E/HIBE88 Data', *Beitr. Phys. Atmosph.* **63**, 85–100.

Sellers, P. J., Mintz, Y., Sud, V. C., and Dalcher, A.: 1986, 'A Simple Model (Si-B) for Use within General Circulation Models', *J. Atm. Sci.* **43**, 505–531.

Sievers, U., Forkel, R., and Zdunkowski, W. G.: 1983, 'Transport Equations for Heat and Moisture in the Soil and their Application to Boundary Layer Problems', *Beitr. Phys. Atmoph.* **56**, 58–83.

Taconet, O., Bernard, R., and Vidal-Madjar, D.: 1986, 'Evapotranspiration over Agriculture Region Using a Surface Flux/Temperature Model based on NOAA-AVHRR Data', *J. Clim. Appl. Meteorol.* **25**, 248–307.

Thom, A. S.: 1972, 'Momentum, Mass and Heat Exchange of Vegetation', *Quart. J. R. Meteorol. Soc.* **98**, 124–134.

Tjernström, M.: 1989, 'Some Tests with a Surface Energy Balance Scheme, Including a Bulk Parameterization for Vegetation, in a Mesoscale Model', *Boundary-Layer Meteorol.* **48**, 33–68.

Yamada T. and Mellor, G. L.: 1975, 'A Simulation of the Wangara Atmospheric Boundary Layer Data', *J. Atm. Sci.* **32**, 2309–2329.

Zdunkowski, W. G., Paegle, J., and Fye, F.: 1975a, 'The Short-Term Influence of Atmospheric Carbon Dioxide on the Temperature Profile in the Boundary Layer', *Pageoph.* **113**, 331–353.

Zdunkowski, W. G., Paegle, J., and Reilly, J.: 1975b, 'The Effect of Soil Moisture upon the Atmospheric and Soil Temperature near the Air-Soil Interface', *Arch. Met. Geoph. Biol., Ser. A.* **24**, 245–268.

Zdunkowski, W. G., Panhans, W.-G., Welch, R., and Korb, G.: 1982, 'A Radiation Scheme for Circulation and Climate Models', *Beitr. Phys. Atmoph.* **55**, 215–238.